

# Etching Silicon with HF–HNO<sub>3</sub>–H<sub>2</sub>SO<sub>4</sub>/H<sub>2</sub>O Mixtures – Unprecedented Formation of Trifluorosilane, Hexafluorodisiloxane, and Si–F Surface Groups

Marcus Lippold,<sup>[a]</sup> Uwe Böhme,<sup>[a]</sup> Christoph Gondek,<sup>[a]</sup> Martin Kronstein,<sup>[a]</sup> Sebastian Patzig-Klein,<sup>[a]</sup> Martin Weser,<sup>[a]</sup> and Edwin Kroke\*<sup>[a]</sup>

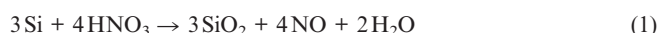
**Keywords:** Silicon / Silanes / Fluorine / Hydrofluoric acid / Wet chemical etching / Surface analysis

The etching behaviour of sulfuric-acid-containing HF–HNO<sub>3</sub> solutions towards crystalline silicon surfaces has been studied over a wide range of H<sub>2</sub>SO<sub>4</sub> concentrations. For mixtures with low sulfuric acid concentration, NO<sub>2</sub>/N<sub>2</sub>O<sub>4</sub>, N<sub>2</sub>O<sub>3</sub>, NO and N<sub>2</sub>O have been detected by means of FTIR spectroscopy. Increasing concentrations of nitric acid lead to high etching rates and to an enhanced formation of NO<sub>2</sub>/N<sub>2</sub>O<sub>4</sub>. Different products were observed for the etching of silicon with sulfuric-acid-rich mixtures [*c*(H<sub>2</sub>SO<sub>4</sub>) > 13 mol L<sup>-1</sup>]. Trifluorosilane and hexafluorodisiloxane were identified by FTIR spectroscopy as additional reaction products. In con-

trast to the commonly accepted wet chemical etching mechanism, the formation of trifluorosilane is not accompanied by the formation of molecular hydrogen (according to Raman spectroscopy). Thermodynamic calculations and direct reactions of F<sub>3</sub>SiH with the etching solution support an intermediate oxidation of trifluorosilane and the formation of hexafluorodisiloxane. The etched silicon surfaces were investigated by diffuse reflection FTIR and X-ray photoelectron spectroscopy (XPS). Surprisingly, no SiH terminations were observed after etching in sulfuric-acid-rich mixtures. Instead, a fluorine-terminated surface was found.

## Introduction

For microelectronic and photovoltaic applications, the etching of silicon surfaces is of enormous technical and economic relevance. The removal of metal impurities from silicon materials, texturing of silicon wafers and recycling of solar cells are realized by wet chemical etching processes.<sup>[1]</sup> In conventional HF–HNO<sub>3</sub>-based mixtures, dissolution of silicon requires the stepwise oxidation of silicon atoms and the formation of water-soluble complexes. According to Robbins and Schwartz, nitric acid produces an intermediate SiO<sub>2</sub> layer [Equation (1)], which is dissolved by hydrofluoric acid [Equation (2)].<sup>[2–4]</sup> The overall reaction is written in Equation (3).

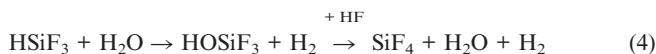


Turner described the mechanism of silicon dissolution as an electrochemical process with local anodic and local cathodic areas on the silicon surface. Corresponding to this

model, the injection of holes (h<sup>+</sup>) in the valence band by nitric acid at cathodic sites is followed by the formation of an intermediate SiO<sub>2</sub> layer, which is dissolved by hydrofluoric acid, at local anodic sites.<sup>[5]</sup> However, X-ray photoelectron spectroscopy (XPS) measurements of etched silicon surfaces exclude the formation of intermediate SiO<sub>2</sub> layers.<sup>[6,7]</sup> Silicon surfaces etched with HF–HNO<sub>3</sub>–H<sub>2</sub>O mixtures are covered by hydrogen-containing –SiH<sub>*x*</sub> (*x* = 1–3) groups. In a few cases partial fluorine coverage has been reported. F-containing groups such as –SiH<sub>2</sub>F and –SiHF<sub>2</sub> were identified by means of real-time, in-situ infrared studies.<sup>[9]</sup> SiH-terminated surfaces are inert against hydrofluoric acid solutions. Only the injection of holes in the valence band by oxidants and their existence on the silicon surface enable an attack by fluoride-containing species.<sup>[10–12]</sup> Therefore, etching rates of hydrogen-terminated silicon bulk material are quite low in hydrofluoric acid without further oxidants (about 0.5 Å min<sup>-1</sup>).<sup>[14]</sup> Recent investigations of acidic etching mixtures support the concept of nitrogen–oxygen cations, as crucial oxidants in the silicon dissolution process.<sup>[1a,15–19]</sup> Nitrous acid HNO<sub>2</sub> and nitrosyl ions NO<sup>+</sup>, intermediates formed by reduction of nitric acid, are strong oxidants of hydrogen-terminated silicon surfaces.<sup>[15]</sup> During the etching of silicon in mixtures with 6 mol L<sup>-1</sup> HF and 6 mol L<sup>-1</sup> HNO<sub>3</sub>, Kooij et al. determined H<sub>2</sub> (80.0%), N<sub>2</sub>O (18.3%), NO (1.0%) and NO<sub>2</sub> (0.7%) as gaseous reaction products.<sup>[20]</sup> The amount of H<sub>2</sub> strongly depends on the HF/HNO<sub>3</sub> ratio. Especially in mixtures with low amounts of nitric acid, hydrogen is generated.<sup>[21]</sup> For etching n-type silicon under strong illumination, the intermediate forma-

[a] Department of Inorganic Chemistry, TU Bergakademie Freiberg, Leipziger Str. 29, 09596 Freiberg, Germany  
 Fax: +49-3731-394058  
 E-mail: edwin.kroke@chemie.tu-freiberg.de  
 Homepage: <http://tu-freiberg.de/fakult2/aoch/agsi/index.html>  
 Supporting information for this article is available on the WWW under <http://dx.doi.org/10.1002/ejic.201200674>.

tion of trifluorosilane HSiF<sub>3</sub> was proposed.<sup>[11]</sup> In aqueous solution, the hydrolysis of HSiF<sub>3</sub> should lead to the formation of hydrogen according to Equation (4).<sup>[12,13,22]</sup>



In the present study the reaction behaviour of crystalline silicon in HF–HNO<sub>3</sub>–H<sub>2</sub>SO<sub>4</sub>/H<sub>2</sub>O etching mixtures is studied. Our investigations are focused on fundamental effects on the silicon dissolution process by the addition of sulfuric acid to conventional HF–HNO<sub>3</sub>-based mixtures. The formation of trifluorosilane, hexafluorodisiloxane and fluorine-terminated silicon surfaces are reported, analyzed and discussed with respect to the solution. A new silicon etching reaction sequence is proposed.

## Results and Discussion

### Gaseous Reaction Products of HF–HNO<sub>3</sub>–H<sub>2</sub>SO<sub>4</sub>/H<sub>2</sub>O Etching Solutions

In HF–HNO<sub>3</sub>-based solutions, silicon etching rates strongly depend on the concentrations of hydrofluoric acid and nitric acid.<sup>[2,23]</sup> Additional components, for example, CH<sub>3</sub>COOH and H<sub>2</sub>SO<sub>4</sub>, influence the reactivity and determine the surface structures of the etched silicon.<sup>[3,19,24,25]</sup> H<sub>2</sub>SO<sub>4</sub>-containing mixtures are highly reactive towards crystalline silicon. Depending on the mixture composition, etching rates up to 4000–5000 nm s<sup>−1</sup> were obtained.<sup>[19]</sup> During silicon etching, nitric acid molecules and several intermediates are reduced at the silicon/electrolyte interface by transfer of electrons (e<sup>−</sup>) from the silicon surface to the oxidation agent or by injection of h<sup>+</sup> into the valence band of the semiconductor. FTIR spectroscopy enables the analysis of gaseous reaction products (Figure 1). Depending on the concentration of nitric acid, different nitrogen oxides are formed. HF–HNO<sub>3</sub>–H<sub>2</sub>SO<sub>4</sub>/H<sub>2</sub>O etching mixtures with constant concentrations of hydrofluoric acid and sulfuric acid and HNO<sub>3</sub> concentrations of 4.3 mol L<sup>−1</sup> lead to the formation of NO<sub>2</sub>, NO and N<sub>2</sub>O. Increasing the nitric acid concentration accelerates the silicon oxidation steps, and the silicon etching rates increase from 30.6 nm s<sup>−1</sup> for 4.3 mol L<sup>−1</sup> HNO<sub>3</sub> to 225.1 nm s<sup>−1</sup> for 7.5 mol L<sup>−1</sup> HNO<sub>3</sub> (Figure 1). For nitric acid concentrations higher than 5.3 mol L<sup>−1</sup>, N<sub>2</sub>O<sub>4</sub> and N<sub>2</sub>O<sub>3</sub> were detected in addition to NO<sub>2</sub>, NO and N<sub>2</sub>O. The assignment of the vibrational bands of the N<sub>x</sub>O<sub>y</sub> species is based on literature data (Table 1).

In HF–HNO<sub>3</sub>–H<sub>2</sub>SO<sub>4</sub>/H<sub>2</sub>O mixtures, increased sulfuric acid concentrations and low water content support the formation of nitronium ions NO<sub>2</sub><sup>+</sup>. According to Equation (5), the equilibrium of undissociated HNO<sub>3</sub> and NO<sub>2</sub><sup>+</sup> is shifted because of the high sulfuric acid concentration.<sup>[19]</sup> According to Equations (6) and (7), the transfer of an electron from the valence band of silicon to a nitric acid molecule or to a nitronium ion reduces these substrates to NO<sub>2</sub>, which partially dimerizes at room temperature to dinitrogen tetroxide N<sub>2</sub>O<sub>4</sub>. Dissolved nitrogen dioxide can be reduced to

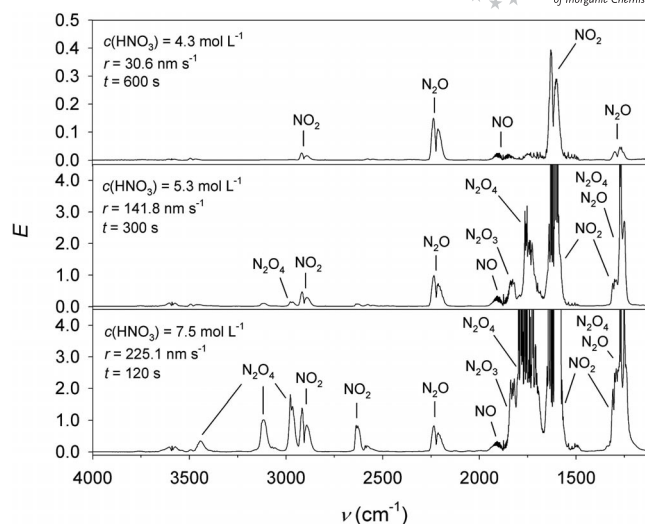
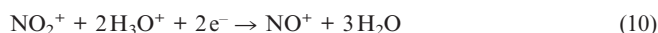
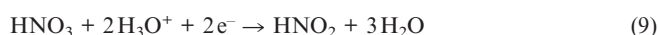
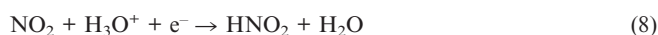
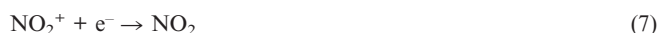


Figure 1. FTIR spectra of gaseous reaction products after dissolving silicon in HF–HNO<sub>3</sub>–H<sub>2</sub>SO<sub>4</sub>/H<sub>2</sub>O etching mixtures. The concentrations of hydrofluoric acid and sulfuric acid were kept constant [*c*(HF) = 5.8 mol L<sup>−1</sup>, *c*(H<sub>2</sub>SO<sub>4</sub>) = 1.1 mol L<sup>−1</sup>].

Table 1. Selected IR vibrations of gaseous N<sub>x</sub>O<sub>y</sub> species [cm<sup>−1</sup>].

Species	Observed	Literature
HNO <sub>3</sub>	3550	3550 <sup>[26,27]</sup>
	1710	1708 <sup>[28]</sup>
	1311	1325 <sup>[28]</sup>
N <sub>2</sub> O <sub>4</sub>	3441	3442 <sup>[26]</sup>
	3116	3117 <sup>[26]</sup>
	2972	2973 <sup>[26]</sup>
	1748	1749 <sup>[26]</sup>
	1260	1261 <sup>[26]</sup>
NO <sub>2</sub>	2905	2906 <sup>[26]</sup>
	2628	2627 <sup>[26]</sup>
	1612	1617 <sup>[26]</sup>
	1324	1320 <sup>[26]</sup>
N <sub>2</sub> O <sub>3</sub>	1827	1830 <sup>[26]</sup>
	1595	1594 <sup>[26]</sup>
	1293	1296 <sup>[26]</sup>
NO	1875	1876 <sup>[26]</sup>
N <sub>2</sub> O	2224	2224 <sup>[26]</sup>
	1288	1284 <sup>[26]</sup>

nitrous acid by a further single electron transfer [Equation (8)]. The simultaneous transfer of two electrons to nitric acid molecules or to nitronium ions should reduce them to N(+3) intermediates according to Equations (9) and (10).



Owing to their high oxidation potentials, intermediate N(+3) species act as additional oxidants of the silicon sur-

face.<sup>[15,16,18]</sup> Thus, nitrous acid is reduced to nitrogen monoxide by a single electron transfer [Equation (11)]. According to Equation (12), the simultaneous transfer of two electrons might reduce N(+3) species to nitroso acid HNO, which can dimerize to hyponitrous acid H<sub>2</sub>N<sub>2</sub>O<sub>2</sub> and finally decompose to nitrous oxide and water [Equation (13)].

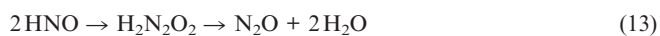
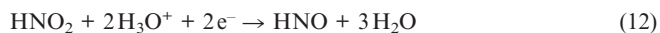


Figure 2a shows the FTIR spectrum of the gaseous reaction products after etching silicon in an HF–HNO<sub>3</sub>–H<sub>2</sub>SO<sub>4</sub> mixture with high concentrations of sulfuric acid and no additional water. NO<sub>2</sub>/N<sub>2</sub>O<sub>4</sub> and N<sub>2</sub>O were identified as reduced nitrogen-containing species. The absence of the prominent  $\nu(\text{NO})$  band of nitrogen monoxide at 1875 cm<sup>-1</sup> indicates that the reduction of N(+3) species in H<sub>2</sub>SO<sub>4</sub>-rich mixtures preferentially proceeds by 2e<sup>-</sup> steps. The vibration band at 2316 cm<sup>-1</sup> can be assigned to the prominent SiH band of trifluorosilane (HSiF<sub>3</sub>).<sup>[28,29]</sup> As mentioned in the Introduction, trifluorosilane was postulated as an intermediate in the electrochemical etching process of n-type silicon under illumination. Until now, the generation of trifluorosilane could not be verified. Even in-situ FTIR spectroscopic investigations provided no evidence for the formation of trifluorosilane.<sup>[30]</sup> In addition to the identification of trifluorosilane, a further silicon-containing gaseous compound was detected. The vibration bands at  $\tilde{\nu} = 1190$ , 1826 and 2054 cm<sup>-1</sup> correspond to hexafluorodisiloxane.<sup>[31]</sup> At-line FTIR spectroscopic measurements clearly indicate the formation of trifluorosilane during the etching of silicon in HF–HNO<sub>3</sub>–H<sub>2</sub>SO<sub>4</sub> mixtures. With increasing reaction times, the intensities of the SiH band decreases (Figure 2b). After 20 min, no trifluorosilane was detected by FTIR spectroscopy. During the etching process, the accumulation of species that react with trifluorosilane or a decrease in species that are essential for the formation of trifluorosilane might be the cause for the time-dependent reaction behaviour. The intensities of the bands of other gaseous species increase until a reaction time of 20 min. The consumption of bath components and the evaporation of hydrofluoric acid as well as nitric acid lead to decreasing reactivities for reaction times longer than 20 min (spectra not shown). Higher HNO<sub>3</sub> concentrations result in lower F<sub>3</sub>SiH amounts and much larger hexafluorodisiloxane concentrations in the gas phase (Figure S1).

According to Equation (4), the hydrolysis of trifluorosilane in aqueous hydrofluoric acid solutions should generate silicon tetrafluoride and molecular hydrogen. In spite of the formation of trifluorosilane, no hydrogen was detectable by means of Raman spectroscopy after etching silicon in H<sub>2</sub>SO<sub>4</sub>-rich etching mixtures (Figure S6), i.e., trifluorosilane is not hydrolyzed according to Equation (4) in the etching mixtures investigated. Low concentrations of free water and hydrofluoric acid should hamper the hydrolysis of trifluorosilane. Several oxidizing agents, e.g., HNO<sub>3</sub>, NO<sub>2</sub><sup>+</sup>,

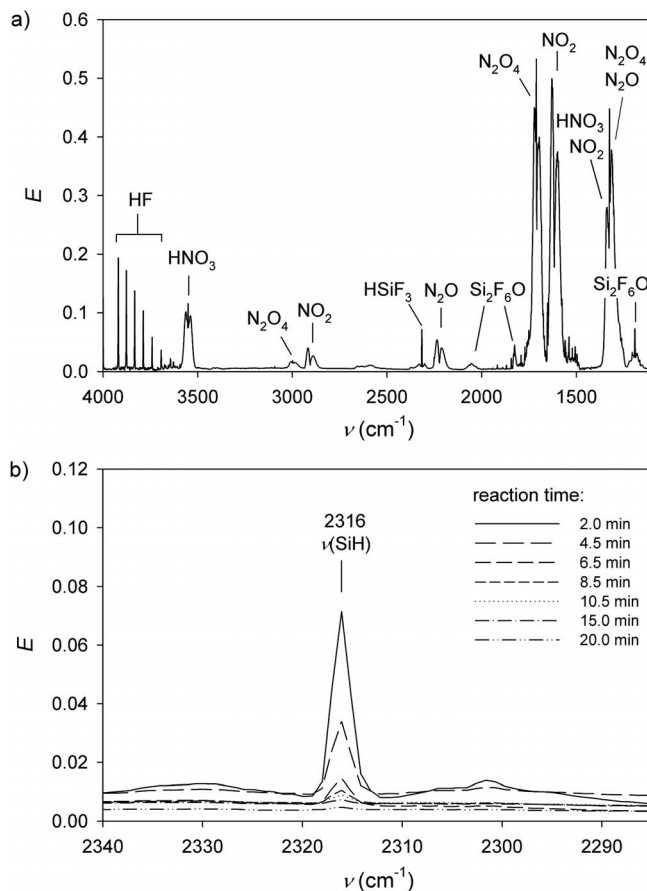
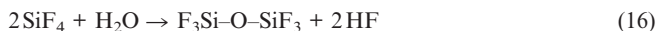


Figure 2. (a) FTIR spectrum of gaseous reaction products after etching silicon in an HF–HNO<sub>3</sub>–H<sub>2</sub>SO<sub>4</sub> mixture. (b) At-line FTIR spectra in the range of the  $\nu(\text{SiH})$  band of trifluorosilane for different reaction times. Mixture composition:  $c(\text{HF}) = 2.3 \text{ mol L}^{-1}$ ,  $c(\text{HNO}_3) = 1.7 \text{ mol L}^{-1}$ ,  $c(\text{H}_2\text{SO}_4) = 15.0 \text{ mol L}^{-1}$  (see also Figure S2).

NO<sub>2</sub> and NO<sup>+</sup>, might lead to the oxidation of trifluorosilane in HF–HNO<sub>3</sub>–H<sub>2</sub>SO<sub>4</sub> etching mixtures. To identify possible reactions of trifluorosilane and to clarify the formation of hexafluorodisiloxane, DFT calculations were carried out to determine the Gibbs free energies of Equations (14), (15) and (16). The negative Gibbs free energy  $\Delta_R G = -265.4 \text{ kJ mol}^{-1}$  for the reaction of trifluorosilane and nitronium ions [Equation (14)] shows that the formation of trifluorosilanol (HOSiF<sub>3</sub>) under thermodynamic considerations is possible. However, there is no spectroscopic evidence for the formation of trifluorosilanol to date. The weak exergonic condensation of two trifluorosilanol molecules according to Equation (15) might be responsible for this and should generate hexafluorodisiloxane ( $\Delta_R G = -0.6 \text{ kJ mol}^{-1}$ ). Additionally, large amounts of sulfuric acid bind the water molecules formed and shift the equilibrium in Equation (15) towards the products. For sulfuric-acid-rich mixtures with HNO<sub>3</sub> concentrations of 8.9 mol L<sup>-1</sup>, intense hexafluorodisiloxane vibration bands indicate a nearly complete oxidation of trifluorosilane to trifluorosilanol followed by condensation according to Equation (15). Increasing concentrations of nitronium ions, as detected in these

solutions<sup>[19]</sup> might be responsible for this observation. The formation of hexafluorodisiloxane is described in the literature to occur by partial hydrolysis of silicon tetrafluoride, according to Equation (16), only at high temperatures.<sup>[32,33]</sup> At room temperature, the calculated positive Gibbs free energy  $\Delta_R G = 54.3 \text{ kJ mol}^{-1}$  does not support the hydrolysis of silicon tetrafluoride in the HF–HNO<sub>3</sub>–H<sub>2</sub>SO<sub>4</sub> etching system.



To confirm the HSiF<sub>3</sub> formation during wet chemical etching and the subsequent generation of F<sub>3</sub>SiOSiF<sub>3</sub>, trifluorosilane was prepared according to Equation (17) by the addition of trichlorosilane to a zinc fluoride/tetrahydrofuran suspension.<sup>[34]</sup> The spectra of the synthesized trifluorosilane and of the gaseous reaction products are shown in Figure 3. The  $\nu(\text{SiH})$  bands at 2316 cm<sup>-1</sup> correspond in both spectra. Because of the intensive bands of further gaseous species (SiF<sub>4</sub>, F<sub>3</sub>SiOSiF<sub>3</sub>, N<sub>x</sub>O<sub>y</sub>), the additional bands of trifluorosilane [ $\nu(\text{SiF}_3) = 992$ ,  $\nu(\text{SiF}) = 858$ ,  $\delta(\text{SiH}) = 844$  and  $\delta(\text{SiF}_3) = 424 \text{ cm}^{-1}$ ] appear as shoulders in the spectrum of the gaseous reaction products. The vibration bands were assigned according to Table 2.

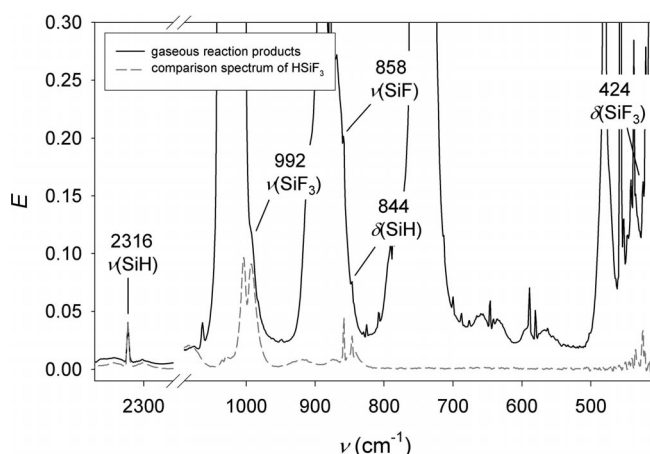
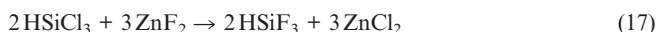


Figure 3. Characteristic vibration bands of trifluorosilane. FTIR spectra of synthesized trifluorosilane (dashed line) and a spectrum of the gaseous reaction products (solid line) after etching silicon in HF–HNO<sub>3</sub>–H<sub>2</sub>SO<sub>4</sub> mixtures [ $c(\text{HF}) = 2.6 \text{ mol L}^{-1}$ ,  $c(\text{HNO}_3) = 3.2 \text{ mol L}^{-1}$ ,  $c(\text{H}_2\text{SO}_4) = 13.5 \text{ mol L}^{-1}$ ,  $t = 120 \text{ s}$ ].

Synthesized trifluorosilane was introduced into a sulfuric-acid-rich etching mixture. After the reaction, the SiH vibration band of trifluorosilane could not be observed in the FTIR spectrum (Figure S3). Instead, bands of hexafluorodisiloxane were detected. Therefore, the calculated Gibbs free energies (vide supra) and experimental data confirm the subsequent oxidation of trifluorosilane, most likely via trifluorosilanol, to form hexafluorodisiloxane. After the

Table 2. Selected IR vibrations of gaseous Si-containing species generated during silicon etching in HF–HNO<sub>3</sub>–H<sub>2</sub>SO<sub>4</sub> mixtures in cm<sup>-1</sup>.

Species	Observed	Literature
HSiF <sub>3</sub>	2316, 2316 <sup>[a]</sup>	2316 <sup>[28,29]</sup>
	992, <sup>[b,c]</sup> 999 <sup>[a]</sup>	998 <sup>[28,29]</sup>
	858, <sup>[b]</sup> 858 <sup>[a]</sup>	858 <sup>[28,29]</sup>
	844, <sup>[b]</sup> 846 <sup>[a]</sup>	844 <sup>[28,29]</sup>
	424, <sup>[b]</sup> 424 <sup>[a]</sup>	425 <sup>[28,29]</sup>
F <sub>3</sub> SiOSiF <sub>3</sub>	2054	2040 <sup>[31]</sup>
	1826	1825 <sup>[31]</sup>
	1190	1200 <sup>[31]</sup>
	1021 <sup>[c]</sup>	1028 <sup>[31]</sup>
SiF <sub>4</sub>	1021 <sup>[c]</sup>	1031 <sup>[31]</sup>

[a] Vibration bands of synthesized HSiF<sub>3</sub>. [b] Vibration bands appear as shoulders. [c] The  $\nu(\text{SiF})$  vibration bands of HSiF<sub>3</sub>, F<sub>3</sub>SiOSiF<sub>3</sub> and SiF<sub>4</sub> interfere.

reaction of trifluorosilane with the sulfuric-acid-rich mixture, the <sup>19</sup>F NMR spectrum of the HF–HNO<sub>3</sub>–H<sub>2</sub>SO<sub>4</sub> solution indicated two intensive signals, which could be assigned to hydrofluoric acid ( $\delta = -147.1 \text{ ppm}$ ) and fluorosulfuric acid ( $\delta = 37.6 \text{ ppm}$ ) (Figure S4). Additionally, a small peak at  $\delta = -147.2 \text{ ppm}$  was observed in the range of the chemical shifts of trifluorosilane ( $\delta = -159.0 \text{ ppm}$ ) and hexafluorodisiloxane ( $\delta = -161.7 \text{ ppm}$ ) (Figure S5).<sup>[35,36]</sup> However, <sup>29</sup>Si NMR spectra of etching solutions, through which trifluorosilane was passed, did not show any signals; this was attributed to the relatively low solubility of the silane and the low sensitivity of the <sup>29</sup>Si nucleus.

### Gaseous Reaction Products for HF–NOHSO<sub>4</sub>–H<sub>2</sub>SO<sub>4</sub> Etching Solutions

HF–NOHSO<sub>4</sub>–H<sub>2</sub>SO<sub>4</sub> solutions serve as model etching systems for HF–HNO<sub>3</sub>-based mixtures. Both etching systems are characterized by low water content, relatively high mixture viscosities and high oxidation potentials. Therefore, a similar silicon dissolution process is expected. The addition of sulfuric acid leads to the stabilization of nitrosyl ions NO<sup>+</sup> according to Equation (18). The use of nitrosyl hydrogensulfate as the oxidizing agent enables systematic reactivity studies of N(+3) species.<sup>[16,18]</sup>



Figure 4 shows the FTIR spectrum of the gaseous reaction products after etching silicon in HF–NOHSO<sub>4</sub>–H<sub>2</sub>SO<sub>4</sub> mixtures with low HF concentration (1.7 mol L<sup>-1</sup>). Nitrogen monoxide ( $\tilde{\nu} = 1875 \text{ cm}^{-1}$ ) and nitrous oxide ( $\tilde{\nu} = 2224 \text{ cm}^{-1}$ ) were identified as the nitrogen-containing products. The transfer of an electron from the silicon surface to a nitrosyl ion reduces this species to NO. A simultaneous transfer of two electrons or the consecutive transfer of two single electrons to NO<sup>+</sup>, protonation, dimerization and dissociation according to Equation (13) should lead to the formation of N<sub>2</sub>O. Similar to that discussed above, the evaporation of hydrofluoric acid ( $\tilde{\nu} = 3693\text{--}3919 \text{ cm}^{-1}$ ) is favoured by high sulfuric acid concentrations. Trifluorosil-



ane ( $\tilde{\nu} = 2316 \text{ cm}^{-1}$ ) is also generated during silicon etching in HF–NOHSO<sub>4</sub>–H<sub>2</sub>SO<sub>4</sub> solutions. In addition, no molecular hydrogen was detected by means of Raman spectroscopy (Figure S7). In both etching systems, similar reaction conditions (low water and hydrofluoric acid concentrations) lead to the formation of trifluorosilane and inhibit hydrolysis according to Equation (4). However, the vibration bands of hexafluorodisiloxane were not detectable in this case. Therefore, the described oxidation of trifluorosilane, followed by the condensation of trifluorosilanol, appears to be inhibited in the HF–NOHSO<sub>4</sub>–H<sub>2</sub>SO<sub>4</sub> mixtures investigated. This may be, because N(+4) and N(+5) species such as NO<sub>2</sub> or NO<sub>2</sub><sup>+</sup> are unlikely to form in these HF–NOHSO<sub>4</sub>–H<sub>2</sub>SO<sub>4</sub> etching solutions.

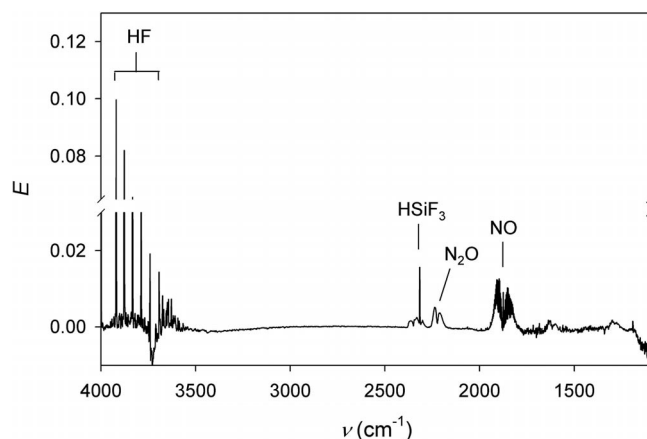


Figure 4. FTIR spectrum of gaseous products after the reaction of silicon with HF–NOHSO<sub>4</sub>–H<sub>2</sub>SO<sub>4</sub>. Mixture composition:  $[c(\text{HF}) = 1.7 \text{ mol L}^{-1}, c(\text{NOHSO}_4) = 1.4 \text{ mol L}^{-1}, c(\text{H}_2\text{SO}_4) = 16.8 \text{ mol L}^{-1}, t = 300 \text{ s}]$ .

### Formation of Si–F Surface Groups

Silicon surfaces etched with HF–HNO<sub>3</sub>–H<sub>2</sub>O mixtures are hydrophobic and hydrogen-terminated. IR spectroscopic investigations confirm the SiH termination. The  $\nu(\text{SiH})$  stretching bands of the relevant SiH and SiH<sub>2</sub> groups are located in the range 2085–2115  $\text{cm}^{-1}$ .<sup>[37]</sup> Figure 5a shows the diffuse reflectance infrared (DR/FTIR) spectrum of an etched multicrystalline silicon surface. The intense band at  $\tilde{\nu} = 2100 \text{ cm}^{-1}$  indicates SiH surface groups. In this sulfuric acid containing etching solution, the concentration of hydrofluoric acid is much higher than the concentration of nitric acid. Etching silicon surfaces in mixtures with low hydrofluoric acid concentrations leads to completely different surface chemistry. Etched silicon surfaces are hydrophilic. On silicon wafers etched in H<sub>2</sub>SO<sub>4</sub>-rich mixtures, no SiH stretching vibrations were detected by DR/FT-IR spectroscopy (Figure 5b). In addition to this, porelike surface textures were observed by means of scanning electron microscopy.<sup>[19]</sup> This disagrees with the principles of silicon dissolution, in which the transport of hydrofluoric acid to the silicon surface is expected to be the rate-limiting process and should lead to the formation of

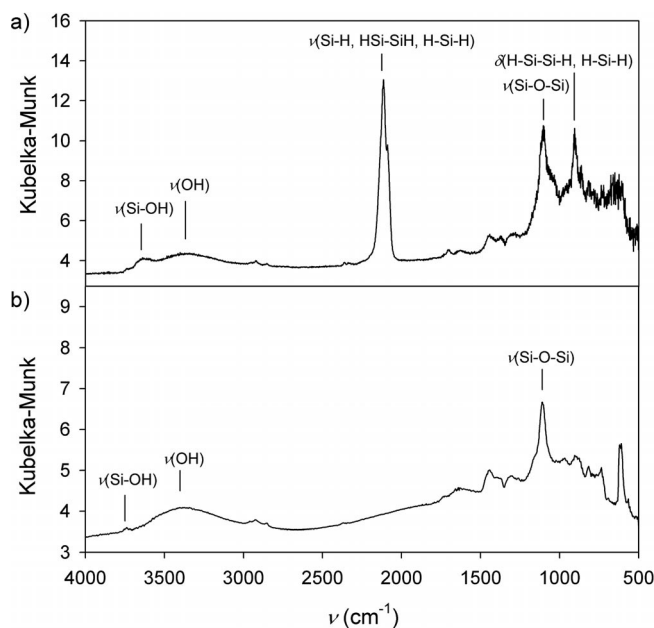


Figure 5. DR/FTIR spectra of etched silicon surfaces. (a) Hydrogen-terminated surface after etching in a HF-rich mixture [ $c(\text{HF}) = 9.0 \text{ mol L}^{-1}, c(\text{HNO}_3) = 1.6 \text{ mol L}^{-1}, c(\text{H}_2\text{SO}_4) = 8.9 \text{ mol L}^{-1}, t = 300 \text{ s}]$ . (b) Silicon surface after etching in a H<sub>2</sub>SO<sub>4</sub>-rich mixture [ $c(\text{HF}) = 2.6 \text{ mol L}^{-1}, c(\text{HNO}_3) = 3.2 \text{ mol L}^{-1}, c(\text{H}_2\text{SO}_4) = 13.5 \text{ mol L}^{-1}, t = 600 \text{ s}]$ .

polished surfaces. In both spectra, the Si–OH vibrations bands at  $\tilde{\nu} \approx 3700 \text{ cm}^{-1}$  support the intermediate existence of Si–F surface species. Rinsing of the etched silicon surfaces with deionized water leads to hydrolysis of the SiF groups [Equation (19)]. The OH-group surface concentration increases with the duration of water rinsing.<sup>[38]</sup>



The XPS spectrum of an etched silicon surface is depicted in Figure 6. The H<sub>2</sub>SO<sub>4</sub>-rich etching solution contains relatively small amounts of hydrofluoric acid [ $c(\text{HF}) = 2.6 \text{ mol L}^{-1}$ ]. In the F 1s region, two peaks were observed. The peak at 686.0 eV corresponds to Si<sub>3–x</sub>SiF<sub>x</sub> surface groups and the second peak at 689.5 eV can be assigned to silicon oxyfluoride species such as (SiO)<sub>3–x</sub>SiF<sub>x</sub>.<sup>[39,40]</sup> Additional peaks for oxygen-containing surface species occur in the O 1s region at 532.3 eV and in the Si 2p region at 102.5 eV. For SiOF suboxides, a binding energy of 102 eV was determined.<sup>[41]</sup> Intensive oxygen coverage should result from the hydrolysis of SiF groups. Therefore, Si–F bonds were formed during the etching of silicon in H<sub>2</sub>SO<sub>4</sub>-rich etching mixtures. In contrast, no oxygen-containing surface species were observed by XPS analysis after etching silicon wafers in HF–HNO<sub>3</sub>–H<sub>2</sub>O mixtures.<sup>[7,8]</sup>

The existence of an SiF-terminated silicon surface and the formation of trifluorosilane during etching in H<sub>2</sub>SO<sub>4</sub>-rich HF–HNO<sub>3</sub>-based mixtures indicate different silicon dissolution steps. Scheme 1 illustrates possible reaction steps on the silicon/electrolyte interface for etching in sulfuric-acid-rich HF–HNO<sub>3</sub>–H<sub>2</sub>SO<sub>4</sub> mixtures. During step (1) of silicon dissolution, the native oxide is etched by hydro-

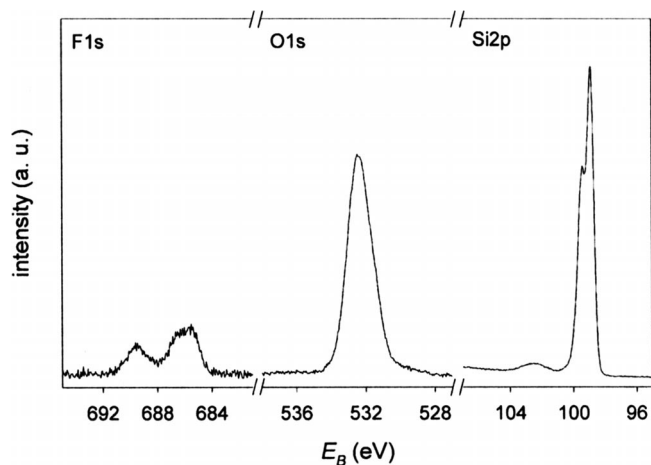
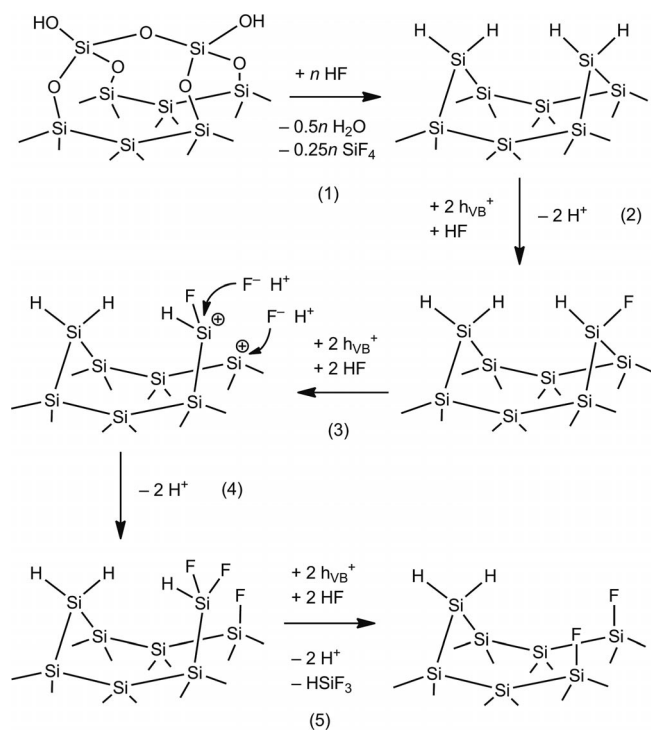


Figure 6. XPS spectrum of a silicon surface etched by a H<sub>2</sub>SO<sub>4</sub>-rich mixture [ $c(\text{HF}) = 2.6 \text{ mol L}^{-1}$ ,  $c(\text{HNO}_3) = 3.2 \text{ mol L}^{-1}$ ,  $c(\text{H}_2\text{SO}_4) = 13.5 \text{ mol L}^{-1}$ ,  $t = 600 \text{ s}$ ].

fluoric acid. The removal of the native oxide generates an intermediate hydrogen coverage. The oxidation of the silicon surface proceeds through reduction of nitrogen-containing species, e.g., HNO<sub>3</sub>, NO<sub>2</sub><sup>+</sup> and NO<sup>+</sup>. Thereby, electrons are transferred from silicon to oxidizing agents by the injection of holes  $h_{\text{VB}}^+$  into the valence band of the semiconductor. In step (2), the injection of holes and their existence near the silicon surface weaken the Si–H bonds and enable the replacement of H atoms by F atoms. The formed Si–F bonds polarize the Si–Si backbonds. This facilitates a subsequent oxidation and the attack of fluoride species to



Scheme 1. Proposed reaction steps for the formation of trifluorosilane and fluorine-covered silicon surfaces during etching in sulfuric-acid-rich HF–HNO<sub>3</sub>–H<sub>2</sub>SO<sub>4</sub> mixtures.

saturate the oxidized silicon atoms. The simultaneous transfer of two electrons (injection of two holes) followed by the reaction with fluoride ions forms a –SiF<sub>2</sub>H group and a fluorine-covered silicon surface atom, see steps (3) and (4). In step (5), the further injection of holes and the reaction with two fluoride species release trifluorosilane and result in a fluoride-covered silicon surface. The fluorine termination of the surface might result from the high oxidation potential and the low concentration of hydrofluoric acid in the etching mixture, i.e., the reaction of fluoride ions with silicon surface atoms is the rate-determining step. Therefore, the reaction behaviour of sulfuric-acid-rich HF–HNO<sub>3</sub>–H<sub>2</sub>SO<sub>4</sub> mixtures differs from the conventional conception of silicon dissolution. For dissolving silicon in aqueous hydrofluoric acid solutions, the injection of holes into the valence band is described as the rate-determining step.<sup>[13]</sup>

## Conclusions

In contrast to the conventional HF–HNO<sub>3</sub>–H<sub>2</sub>O etching system, sulfuric-acid-containing mixtures exhibit a varying etching behaviour. This is clearly indicated by thorough analysis of the gaseous reaction products by FTIR and Raman spectroscopy as well as investigation of the etched silicon surfaces with DR/FTIR and XPS. During the etching of silicon in H<sub>2</sub>SO<sub>4</sub>-rich mixtures, trifluorosilane, hexafluorodisiloxane and fluorine-terminated surfaces are formed in contrast to SiF<sub>4</sub> (and H<sub>2</sub>SiF<sub>6</sub>) and hydrogen-terminated surfaces, as usually found. Fundamental studies of the HF–HNO<sub>3</sub>–H<sub>2</sub>SO<sub>4</sub> etching system indicate an intermediate oxidation of trifluorosilane most likely to trifluorosilanol by nitric acid or nitronium ions, followed by condensation of HOSiF<sub>3</sub> to form hexafluorodisiloxane. Silicon wafers etched by H<sub>2</sub>SO<sub>4</sub>-rich mixtures exhibit a completely different surface situation as shown by the absence of the prominent SiH band. XPS analysis of a freshly etched silicon surface indicates peaks that prove the existence of Si–F surface groups. However, the basic oxidation step corresponds to the well-established reaction mechanism of silicon dissolution in HF-containing mixtures, which is based on the removal of electrons from the Si–Si bonds instead of the Si–H surface moieties. This is supported by the absence of molecular hydrogen and also the formation of trifluorosilane. The unprecedented surface chemistry results from different silicon dissolution steps.

Further spectroscopic investigations of intermediates in HF–HNO<sub>3</sub>–H<sub>2</sub>SO<sub>4</sub> etching solutions should clarify single reaction steps, especially the oxidation of Si–H surface groups by NO<sub>x</sub><sup>+</sup> at the silicon/electrolyte interface. Reactivity studies of trifluorosilane towards several bath components should provide an indication of the formation of molecular hydrogen during etching silicon in conventional HF–HNO<sub>3</sub>–H<sub>2</sub>O mixtures.

## Experimental Section

**Etching Mixtures:** **Caution:** Suitable safety precautions have to be taken into account when performing etching experiments with hy-

drofluoric acid. All experiments were performed in an HF-approved fume hood and with HF-approved laboratory equipment.

HF–HNO<sub>3</sub>–H<sub>2</sub>SO<sub>4</sub> etching solution (25 mL) was prepared by adding freshly distilled nitric acid (100 wt.-%) and analytical-grade hydrofluoric acid (40 wt.-%) dropwise to analytical-grade sulfuric acid (97 wt.-%) in a PP beaker with ice/NaCl cooling. To distill nitric acid, sulfuric acid (200 mL, 97 wt.-%) was added to analytical-grade nitric acid (100 mL, 65 wt.-%) with cooling. The mixture was heated slowly and distilled at 2 kPa. After adding double the volume of sulfuric acid to the distillate, the mixture was distilled again.

HF–NOHSO<sub>4</sub>–H<sub>2</sub>SO<sub>4</sub> etching mixtures were prepared by dissolving nitrosyl hydrogensulfate in analytical-grade sulfuric acid (97 wt.-%) and adding hydrofluoric acid (40 wt.-%). Nitrosyl hydrogensulfate was synthesized by bubbling dried SO<sub>2</sub> into fuming nitric acid (100 mL, 2.4 mol) for several hours, followed by filtration and rinsing with glacial acetic acid and tetrachloromethane under argon. <sup>14</sup>N NMR (H<sub>2</sub>SO<sub>4</sub>): δ = 11.4 ppm. Raman (solid): ν̄ = 414 [ρ(SO<sub>3</sub>)], 571 [δ<sub>s</sub>(SO<sub>3</sub>)], 597 [δ<sub>as</sub>(SO<sub>3</sub>)], 871 [ν(SOH)], 1031 [ν<sub>s</sub>(SO<sub>3</sub>)], 1170 [ν<sub>as</sub>(SO<sub>3</sub>)], 2275 [ν(NO)] cm<sup>-1</sup>.

**Trifluorosilane:** Because of the rapid hydrolysis of HSiF<sub>3</sub>, the following manipulations were carried out under argon. In a three-necked flask, trichlorosilane (4.74 g, 35 mmol) was added dropwise to a suspension of zinc fluoride (10.3 g, 0.10 mol) and tetrahydrofuran (50 mL) with ice/NaCl cooling. To ensure complete reaction of the trichlorosilane, the evolved gas was bubbled through a second three-necked-flask with a suspension of zinc fluoride (5.0 g, 48 mmol) and tetrahydrofuran (40 mL) at room temperature. The trifluorosilane was condensed in a 200 mL Schlenk flask. IR (gas phase): ν̄ = 424 [δ<sub>s</sub>(SiF<sub>3</sub>)], 846 [δ(SiH)], 858 [ν<sub>s</sub>(Si–F)], 998 [ν(SiF<sub>3</sub>)], 2316 [ν(SiH)] cm<sup>-1</sup>.

**Etching Procedure and Characterization:** In a 100 mL Teflon three-necked-flask, multicrystalline silicon wafer pieces (0.2 g, 7 mmol, as-cut, boron doped, thickness 330 μm, resistivity 0.5–2 Ωcm<sup>-1</sup>, Deutsche Solar AG Freiberg) were added to freshly prepared etching mixture (25 mL). To avoid oxidation of nitrogen oxides and hydrolysis of trifluorosilane, all etching experiments were performed under argon. Depending on the reactivity of the etching mixture, the reaction time for each experiment varied from 120 to 600 s. Gaseous reaction products were transferred into an IR gas cell (Thermo Fisher Scientific; d = 10 cm; window material: CaF<sub>2</sub>, KBr) by using Schlenk techniques. The IR spectra were collected with a Nicolet 380 FTIR spectrometer (Thermo Electron Corporation). For Raman spectroscopic investigations, a glass cuvette was used with a T64000 spectrometer (Jobin Yvon). For XPS measurements the etched silicon wafers were rinsed with deionized water and dried immediately. Thereby, brief contact with air could not be avoided. A Specs Phoibos 150 MCD-9 spectrometer was used for XPS measurements with an Al-K<sub>α</sub> source (1486.6 eV) in a vacuum of 8 × 10<sup>-9</sup> mbar.

The <sup>19</sup>F NMR measurements of the etching solutions were performed with a Bruker DPX-400 spectrometer and Teflon inserts. CCl<sub>3</sub>F was used as a standard (376.50 MHz).

**Calculations of Reaction Energies:** DFT calculations were carried out with Gaussian 09.<sup>[42]</sup> The geometries of the molecules under investigation were fully optimized at the DFT level, using Becke's three-parameter hybrid exchange functional, the correlation functional of Lee, Yang and Parr (B3LYP),<sup>[43,44]</sup> and the 6-311+G-(2d,p)<sup>[45–48]</sup> basis set for all atoms. The force constant matrix was computed for all molecules in order to establish the character of the stationary points as minima with zero imaginary frequencies.

The obtained harmonic frequencies were combined with standard statistical thermodynamics to calculate Gibbs free energies at 298.15 K and 1 atm, which allow better comparison with experimental data. Values of Gibbs free energies (*G*), sum of electronic and thermal enthalpies (*H*) and sum of electronic and zero-point energies (*E* + ZPE) are listed in the Supporting Information.

**Supporting Information** (see footnote on the first page of this article): FTIR, <sup>19</sup>F NMR and Raman spectra, list of calculated energies, SEM images.

## Acknowledgments

The authors gratefully acknowledge Prof. Dr. Gerhard Roewer for his useful discussions. Dipl.-Chem. Tobias Weling is acknowledged for collecting the XPS spectra. This work was performed within the Cluster of Excellence “Structure Design of Novel High-Performance Materials via Atomic Design and Defect Engineering (ADDE)” that is financially supported by the European Union (European regional development fund) and by the Ministry of Science and Art of Saxony.

- [1] a) I. Röver, G. Roewer, S. Patzig, W. Weinreich, K. Bohmhammel, *Silicon for the Chemical Industry*, The Norwegian University of Science and Technology, Trondheim **2004**, pp. 319–330; b) S. Wolf, R. N. Tauber, *Silicon Processing for the VLSI Era: Volume 1 – Process Technology*, Lattice Press, Sunset Beach, **1986**; c) H. Löwe, P. Keppel, D. Zach, *Halbleiterätzverfahren*, Akademie-Verlag, Berlin, **1990**; d) W. Kern (Ed.), *Handbook of Semiconductor Wafer Cleaning Technology – Science Technology and Applications*, Noyes Publications, Park Ridge, **1993**.
- [2] H. Robbins, B. Schwartz, *J. Electrochem. Soc.* **1959**, *106*, 505–508.
- [3] H. Robbins, B. Schwartz, *J. Electrochem. Soc.* **1960**, *107*, 108–111.
- [4] B. Schwartz, H. Robbins, *J. Electrochem. Soc.* **1961**, *108*, 365–372.
- [5] D. R. Turner, *J. Electrochem. Soc.* **1960**, *107*, 810–816.
- [6] R. Zanoni, G. Righini, G. Mattogno, L. Schirone, G. Sotgiu, F. Rallo, *J. Lumin.* **1998**, *80*, 159–162.
- [7] M. Steinert, J. Acker, M. Krause, S. Oswald, K. Wetzig, *J. Phys. Chem. B* **2006**, *110*, 11377–11382.
- [8] M. Steinert, J. Acker, S. Oswald, K. Wetzig, *J. Phys. Chem. C* **2007**, *111*, 2133–2140.
- [9] M. Niwano, T. Miura, Y. Kimura, R. Tajima, N. Miyamoto, *J. Appl. Phys.* **1996**, *79*, 3708–3713.
- [10] H. Gerischer, P. Allongue, V. Costa Kieling, *Ber. Bunsen-Ges.* **1993**, *97*, 753–757.
- [11] E. S. Kooij, D. Vanmaekelbergh, *J. Electrochem. Soc.* **1997**, *144*, 1296–1301.
- [12] K. W. Kolasinski, *Phys. Chem. Chem. Phys.* **2003**, *5*, 1270–1278.
- [13] K. W. Kolasinski, *Surf. Sci.* **2009**, *603*, 1904–1911.
- [14] A. Halimaoui, *Surf. Sci.* **1994**, *306*, L550–L554.
- [15] M. T. Kelly, J. K. M. Chun, A. B. Bocarsly, *Appl. Phys. Lett.* **1994**, *63*, 1693–1695.
- [16] S. Patzig, G. Roewer, E. Kroke, I. Röver, *Z. Naturforsch. B* **2007**, *62*, 1411–1421.
- [17] M. Steinert, J. Acker, K. Wetzig, *J. Phys. Chem. C* **2008**, *112*, 14139–14144.
- [18] S. Patzig-Klein, G. Roewer, E. Kroke, *Mater. Sci. Semicond. Process.* **2010**, *13*, 71–79.
- [19] M. Lippold, S. Patzig-Klein, E. Kroke, *Z. Naturforsch. B* **2011**, *66*, 155–163.
- [20] E. S. Kooij, K. Butter, J. J. Kelly, *Electrochem. Solid-State Lett.* **1999**, *2*, 178–180.
- [21] V. Hoffmann, M. Steinert, J. Acker, *J. Anal. At. Spectrom.* **2011**, *26*, 1990–1996.

- [22] K. W. Kolasinski, *J. Phys. Chem. C* **2010**, *114*, 22098–22105.
- [23] I. Röver, G. Roewer, K. Bohmhammel, K. Wambach, *Freiberg. Forschungsh. B* **2004**, *327*, 179–193.
- [24] A. Kübelbeck, C. Zielinski, T. Gölzenleuchter, *DE19962136A1*, **1999**.
- [25] I. Melnyk, P. Fath, *DE102007004060A1*, **2007**.
- [26] F. Melen, M. Hermann, *J. Phys. Chem. Ref. Data* **1992**, *21*, 831–881.
- [27] C. A. Cantrell, J. A. Davidson, A. H. McDaniel, R. E. Shetter, J. G. Calvert, *Chem. Phys. Lett.* **1988**, *148*, 358–363.
- [28] T. Shimanouchi, *J. Phys. Chem. Ref. Data* **1977**, *6*, 993–1102.
- [29] H. Bürger, S. Biedermann, A. Ruoff, *Spectrochim. Acta Part A* **1971**, *27*, 1687–1702.
- [30] A. Venkateswara Rao, F. Ozanam, J.-N. Chazalviel, *J. Electrochem. Soc.* **1991**, *138*, 153–159.
- [31] W. D. Reents, D. L. Wood, A. M. Moujsce, *Anal. Chem.* **1985**, *57*, 104–109.
- [32] J. L. Margrave, K. G. Sharp, P. W. Wilson, *J. Am. Chem. Soc.* **1970**, *92*, 1530–1532.
- [33] P. G. Sennikov, M. A. Ikrin, S. K. Ignatov, A. A. Bagatur'yants, E. Y. Klimov, *Russ. Chem. Bull.* **1999**, *48*, 93–97.
- [34] N. Okada, T. Otsuka, *DE3611983A1*, **1986**.
- [35] B. A. Suvorov, *Russ. J. Gen. Chem.* **2006**, *76*, 1401–1406.
- [36] H. Beckers, H. Bürger, *Z. Anorg. Allg. Chem.* **2001**, *627*, 1217–1224.
- [37] Y. J. Chabal, A. L. Harris, K. Raghavachari, J. C. Tully, *Int. J. Mod. Phys. B* **1993**, *7*, 1031–1078.
- [38] D. Gräf, M. Grundner, R. Schulz, *J. Vac. Sci. Technol. A* **1989**, *7*, 808–813.
- [39] T. Takahagi, A. Ishitani, H. Kuroda, Y. Nagasawa, *J. Appl. Phys.* **1991**, *69*, 803–807.
- [40] C. T. Duncan, A. V. Biradar, S. Rangan, R. E. Mishler, T. Asefa, *Chem. Mater.* **2010**, *22*, 4950–4963.
- [41] J. Pereira, L. E. Pichon, R. Dussart, C. Cardinaud, C. Y. Dularard, E. H. Oubensaid, P. Lefauchaux, M. Boufnichel, P. Ranson, *Appl. Phys. Lett.* **2009**, *94*, 071501/1–071501/3.
- [42] M. J. Frisch, G. W. Trucks, H. B. Schlegel, G. E. Scuseria, M. A. Robb, J. R. Cheeseman, G. Scalmani, V. Barone, B. Mennucci, G. A. Petersson, H. Nakatsuji, M. Caricato, X. Li, H. P. Hratchian, A. F. Izmaylov, J. Bloino, G. Zheng, J. L. Sonnenberg, M. Hada, M. Ehara, K. Toyota, R. Fukuda, J. Hasegawa, M. Ishida, T. Nakajima, Y. Honda, O. Kitao, H. Nakai, T. Vreven, J. A. Montgomery Jr., J. E. Peralta, F. Ogliaro, M. Bearpark, J. J. Heyd, E. Brothers, K. N. Kudin, V. N. Staroverov, T. Keith, R. Kobayashi, J. Normand, K. Raghavachari, A. Rendell, J. C. Burant, S. S. Iyengar, J. Tomasi, M. Cossi, N. Rega, J. M. Millam, M. Klene, J. E. Knox, J. B. Cross, V. Bakken, C. Adamo, J. Jaramillo, R. Gomperts, R. E. Stratmann, O. Yazyev, A. J. Austin, R. Cammi, C. Pomelli, J. W. Ochterski, R. L. Martin, K. Morokuma, V. G. Zakrzewski, G. A. Voth, P. Salvador, J. J. Dannenberg, S. Dapprich, A. D. Daniels, O. Farkas, J. B. Foresman, J. V. Ortiz, J. Cioslowski, D. J. Fox, *Gaussian 09*, Revision B.01, Gaussian, Inc., Wallingford, CT, **2010**.
- [43] A. D. Becke, *J. Chem. Phys.* **1993**, *98*, 5648–5652.
- [44] P. J. Stevens, F. J. Devlin, C. F. Chabalowski, M. J. Frisch, *J. Phys. Chem.* **1994**, *98*, 11623–11627.
- [45] R. Krishnan, J. S. Binkley, R. Seeger, J. A. Pople, *J. Chem. Phys.* **1980**, *72*, 650–654.
- [46] A. D. McLean, G. S. Chandler, *J. Chem. Phys.* **1980**, *72*, 5639–5648.
- [47] M. J. Frisch, J. A. Pople, J. S. Binkley, *J. Chem. Phys.* **1984**, *80*, 3265–3269.
- [48] T. Clark, J. Chandrasekhar, G. W. Spitznagel, P. v. R. Schleyer, *J. Comput. Chem.* **1983**, *4*, 294–301.

Received: June 20, 2012

Published Online: October 8, 2012